PHILOSOPHICAL TRANSACTIONS OF THE ROYAL SOCIETY A MATHEMATICAL, PHYSICAL & ENGINEERING SCIENCES

Waves in the Lee of a Mountain with Elliptical Contours

G. D. Crapper

Phil. Trans. R. Soc. Lond. A 1962 **254**, 601-623
doi: 10.1098/rsta.1962.0007

WAVES IN THE LEE OF A MOUNTAIN WITH ELLIPTICAL CONTOURS

By G. D. CRAPPER

Department of Mathematics, University of Leeds

(*Communicated by M. J. Lighthill, F.R.S.—Received* 28 *September* 1961)

CONTENTS

This paper considers the flow over a mountain which has elliptical contours, for two types of undisturbed air stream. In the first case the static stability parameter $l^2 = g\beta/V^2$ is assumed to be constant throughout the atmosphere, and in the second l^2 is assumed to fall off exponentially with height, in each case with $(V''/V) = q^2$ also being constant. On the basis of the wave equation derived in an earlier paper, a simpler method is developed to find approximations to the difficult Fourier integrals which arise.

The results show that when l^2 is constant the form of the waves is determined by the value of q. When $q = 0$ the waves lie in a strip in the lee of the highest part of the mountain, but when q is large enough the waves are contained in a wedge, and resemble ship waves. When l^2 falls off exponentially the waves closely resemble ship waves for any value of q.

The variation of the amplitude of the waves as various parameters are changed is discussed in detail.

1. Introduction

This paper extends the work of a previous paper, Crapper (1959*a*), which will be referred to as I. The previous paper considers the flow over a mountain with circular contours when the static stability parameter $l^2 = g\beta/V^2$ (see §2 for symbols) is constant throughout the whole depth of the atmosphere. The present paper extends this in three ways: the mountain is allowed to have elliptical contours; the parameter $(V''/V) = q^2$ is allowed to have a non-zero value, although q must be constant; and a more realistic form is used for the l^2 parameter, l^2 decreasing exponentially with height. Further discussion of the case of constant l^2 is also included. The exponential form of l^2 was first used by Palm & Foldvik (1960), in an important paper on two-dimensional waves in the lee of an infinite ridge. They showed that the flow produced when complicated functions, based on actual measured results, are used for l^2 is almost identical at low levels with the flow produced when l^2 is exponential, provided that the rate of fall-off and the initial value of l^2 are chosen suitably. This simple form of l^2 is therefore ideal for an attempt at a three-dimensional solution.

Most of the more important papers on the topic of lee waves which were published before 1959 were discussed in I (§1) and require no further space here. However, there are two such papers of which the author was unaware at the time of publication of I, by Wurtele (1957) and Palm (1958). Wurtele considers the three-dimensional problem of the flow in the lee of a disturbance which is exactly the 'line of doublets' of I (i.e. a disturbance lying along a finite length of a horizontal line perpendicular to the undisturbed air stream), when l^2 is constant. The results of Wurtele's paper and of I agree, but I also shows that the amplitude of the lee waves is much smaller, and the shape of the wave crests different, when a form of disturbance more representative of a mountain is used.

Palm (1958) deals with both two- and three-dimensional waves in an air stream divided into layers, in each of which l^2 is constant, with l^2 decreasing as height increases. This is the form of air stream introduced by Scorer (1949). Palm's three-dimensional problem is exactly that of Scorer & Wilkinson (1956), referred to in I, and the results are similar; in each case numerical methods are used.

A recent paper by Sawyer (1960) gives a numerical solution of the two-dimensional problem which is particularly interesting because the use of an electronic computer enables Sawyer to take various forms for the l^2 parameter which are not confined to well-behaved mathematical functions, and which can therefore be derived from actual potential temperature and velocity profiles of air streams which are known to have given lee waves. The results of earlier theoretical papers are checked by the numerical method, and there is good agreement.

All the theories referred to in I, together with those of Wurtele (1957), Palm (1958) and Sawyer (1960), and I itself, are linear theories, so that their results apply only to the flow over a mountain whose height is small compared with its width. Several recent papers which discuss the two-dimensional problem have presented non-linear theories (Long 1953, 1955; Scorer & Klieforth 1959; Palm & Foldvik 1960; Yih 1960*a*, *b*, *c*), partly with the object of finding conditions under which rotors are formed. Rotors are regions of flow in which the streamlines are closed circuits, and they are found under the crests of lee waves of large amplitude. In three dimensions, however, the linear theory is hardly complete, and non-linear theories have not been attempted.

The present paper is still restricted to a linear theory, and starts from the wave equation derived in I by a double Fourier-transform technique. This equation is solved in §2 for each of the cases of constant l^2 and of exponential l^2, and §2 also contains some further discussion of the problem of the second boundary condition, which is still the subject of controversy. The inverse Fourier transforms, which give the final solution for the streamlines, are dealt with in §3 for constant l^2 and in §4 for exponential l^2. The method used for these integrals has been developed from the method of Lighthill (1960). Approximations are made for large values of x, the distance downstream of the mountain, and in most cases the method of steepest descents is used for the second integration.

The results of §3 show that when l^2 is constant the form of the waves depends on the value of $(V''/V) = q^2$ (= constant). When $q = 0$ the results of I, which was restricted to this case, are confirmed. Perhaps the most surprising of these is that the amplitude of waves in the central plane downstream of the peak of a narrow mountain is greater than the amplitude of the two-dimensional waves in the lee of an infinite ridge of the same cross-section. The amplitude decays downstream as $x^{-\frac{3}{2}}$ for both the two- and three-dimensional cases, but increases linearly with height. The waves are contained in a strip in the lee of the highest part of the mountain. For $q \neq 0$ the solution is not given in detail, but if q is sufficiently large the waves appear to be contained in a wedge, after the manner of ship waves, and for a narrow mountain the decay of wave amplitude downstream is more rapid, as $x^{-\frac{5}{2}}$.

When l^2 is exponential (§4) the value of q has no such significant effect; the waves in the lee of the elliptical mountain are contained in a wedge, whatever the value of q. The waves have maximum amplitude at a finite height, above which the amplitude falls off rapidly. The rate of decay downstream varies from $x^{-\frac{1}{2}}$ for a mountain of small width perpendicular to the air stream, to no decay at all for an infinite ridge. The amplitude increases as the width of the mountain perpendicular to the air stream increases. Mathematically, the difference between the solutions of §§3 and 4 is that the waves of §3 come from branch points of the integrand, while those of §4 come from poles.

These results confirm that a sufficiently rapid decrease of l^2 with height leads to large-amplitude lee waves at low levels. When l^2 is constant the amplitude is small at low levels but may well be important higher up.

2. Solutions of the wave equation

The wave equation is

$$w_0''-w_0'\left\{\frac{g}{c^2}+\beta\right\}+w_0\left\{\frac{k^2l^2}{\xi^2}-k^2-\frac{V''(z)}{V(z)}\right\}=0, \tag{1}$$

where w_0 is defined by

$$w(x,y,z)=\int_{-\infty}^{\infty}\int_{-\infty}^{\infty}\exp\{\mathrm{i}\,(\xi x+\eta y)\}\,w_0(z,\xi,\eta)\,\mathrm{d}\xi\,\mathrm{d}\eta, \tag{2}$$

$w(x,y,z)$ being the small vertical velocity in the disturbed region. Equation (1) was derived from the linearized steady flow equations, neglecting the effects of viscosity, in the previous paper, I. The notation is as follows: x, y are horizontal co-ordinates along and perpendicular to the direction of the undisturbed air stream $V(z)$, and z is the co-ordinate vertically upwards, with the ground at $z=0$; $k=\sqrt{(\xi^2+\eta^2)}$; $l^2=g\beta/V^2(z)$, where $\beta=\beta(z)$ is a parameter depending on the static stability of the atmosphere and g is the acceleration due to gravity; $c=c(z)$ is the speed of sound; primes denote differentiation with respect to z. If we write

$$w_0^*=\left\{\frac{\rho(z)}{\rho(0)}\right\}^{\frac{1}{2}}w_0, \tag{3}$$

where $\rho(z)$ is the density of the air, and use the fact that

$$\frac{g}{c^2}+\beta+\frac{\rho'}{\rho}=0, \tag{4}$$

(1) becomes

$$(w_0^*)''+w_0^*\left\{\frac{k^2l^2}{\xi^2}-k^2-\frac{V''}{V}+\frac{1}{4}\frac{\rho'^2}{\rho^2}-\frac{1}{2}\frac{\rho''}{\rho}\right\}=0. \tag{5}$$

The last two terms of the bracket are small compared with l^2, and we will neglect them.

If ζ is the vertical displacement of a streamline from its undisturbed position,

$$\zeta=\int\frac{w}{V(z)}\,\mathrm{d}x=\frac{1}{V(z)}\int w\,\mathrm{d}x, \tag{6}$$

and therefore $V(z)\,(\rho(z)/\rho(0))^{\frac{1}{2}}\zeta_0$ is also a solution of (5), ζ_0 being the Fourier transform of ζ, defined in the same way as w_0 (2). Thus we can derive the streamline displacement

73-2

directly. We shall leave out the non-dimensional factor $(\rho(z)/\rho(0))^{\frac{1}{2}}$ until the final result. This factor is in any case nearly unity, and some authors in this field have omitted it altogether.

At this stage we must specify l^2 and V''/V as functions of z in such a way that (5) can be solved in a reasonably simple form, so that the inverse transformation which gives ζ will not be too complicated. The cases we shall consider here are (*a*)

$$l^2 = \text{constant}, \quad (V''/V) = q^2 = \text{constant} \tag{7}$$

throughout the atmosphere, and (*b*)

$$l^2 = L^2\,\mathrm{e}^{-2z/h}, \quad (V''/V) = q^2 = \text{constant} \tag{8}$$

throughout the atmosphere. Here L, h and q are all real positive constants, and q may be zero. If $q = 0$, the velocity profile in (7) or (8) is of the form

$$V = U + U'z, \tag{9}$$

U and U' being constants. If $q \neq 0$ the velocity profile is

$$V = U_1\,\mathrm{e}^{+qz} + U_2\,\mathrm{e}^{-qz}, \tag{10}$$

where U_1 and U_2 are constants.

The waves in the lee of a mountain with circular contours were found for case (*a*) with $q = 0$ in I, and in §3 of this paper that solution is extended (by a simplified method) to find the waves in the lee of the mountain given by

$$\zeta(x, y, 0) = H\exp\left\{-\frac{x^2}{a^2} - \frac{y^2}{b^2}\right\}. \tag{11}$$

This mountain has maximum height H, and a is its half-width in the plane $y = 0$ at height $H\mathrm{e}^{-1}$, while b is its half-width in the plane $x = 0$ at the same height; its contours are ellipses with their principal axes in the planes $x = 0$ and $y = 0$.

The waves given by case (*a*) have some remarkable properties, as we shall see below, although it is not a particularly realistic case, since l^2 will never be strictly constant in the atmosphere. Case (*b*) was introduced by Palm & Foldvik (1960), for reasons described in §1. As their problem is two-dimensional, Palm & Foldvik use an exponential form for

$$\frac{g\beta}{V^2} - \frac{V''}{V}, \tag{12}$$

i.e. the present $l^2 - q^2$, and therefore they do not have to define q^2 separately. However, the form of V in (10) with $U_2 = 0$ and q small is similar to the velocity profile which they use in finding their original values of (12), and we can therefore expect case (*b*) to give lee waves of large amplitude at low levels, in the same way as the two-dimensional solution.

Equation (5) (neglecting the last two terms of the bracket) can be solved directly for case (*a*), and by a suitable transformation for case (*b*).

Case (*a*) gives

$$V\zeta_0 = A_1\,\mathrm{e}^{-Kz} + B_1\,\mathrm{e}^{Kz}, \tag{13}$$

where A_1, B_1 are constants and

$$K = \{k^2 + q^2 - k^2 l^2/\xi^2\}^{\frac{1}{2}}. \tag{14}$$

We take the particular solution with $B_1 = 0$, since then $\zeta_0 \to 0$ as $z \to \infty$ when K is real,

$$V\zeta_0 = A_1 \mathrm{e}^{-Kz}. \tag{15}$$

The mountain shape (11) is the streamline at $z = 0$, so that

$$A_1 = V(0)\,\zeta_0(0, \xi, \eta) = \frac{HabV(0)}{4\pi} \exp\left(-\tfrac{1}{4}a^2\xi^2 - \tfrac{1}{4}b^2\eta^2\right), \tag{16}$$

and we have

$$\zeta = \frac{HabV(0)}{4\pi V(z)} \int_{-\infty}^{\infty}\int_{-\infty}^{\infty} \exp\left[\mathrm{i}(\xi x + \eta y) - z\{(\xi^2 - l^2)(1 + \eta^2/\xi^2) + q^2\}^{\frac{1}{2}} - \tfrac{1}{4}a^2\xi^2 - \tfrac{1}{4}b^2\eta^2\right] \mathrm{d}\xi\,\mathrm{d}\eta. \tag{17}$$

The form which (15) takes when K is imaginary depends on the 'upper' boundary condition, and will be derived as in I. There the conditions of time dependence, eventually reaching the steady state as time $\to \infty$, or of small Rayleigh friction terms, lead simply to the condition that the contour of the ξ-integration must pass 'below' the singularities on the real axis of the ξ-plane, in order to give no waves upstream of the mountain.

If we take, for the moment, $q = 0$ in (17) there are singularities at $\xi = \pm l$, and others may appear if the η-integration is carried out first, as in I. Our boundary condition implies that

$$\left.\begin{aligned} \surd(\xi^2 - l^2) &= -\mathrm{i}\surd(l^2 - \xi^2) \quad (0 < \xi < l), \\ &= +\mathrm{i}\surd(l^2 - \xi^2) \quad (-l < \xi < 0). \end{aligned}\right\} \tag{18}$$

The result (18) is the same as that of many previous authors writing on lee waves, including similar problems on water waves: Höiland (1951), Stoker (1953) and Wurtele (1955) work out the time-dependent solution in detail for surface waves, and Palm (1953), Wurtele (1953) do the same for mountain waves; Eliassen & Palm (1954) arrive at the same result by applying a radiation condition; and Corby & Sawyer (1958*a*) assume that the atmosphere has a rigid upper boundary, eventually letting the height of this boundary become infinite. The fact that these various methods all give the same result gives weight to the choice of this condition.

However, Scorer, in his numerous papers, does not use the boundary condition put forward here. Instead he says (Scorer 1958*a*): 'In the absence of a special second condition waves corresponding to no disturbance at the ground should be excluded for the same reason that lee waves on the upstream side of the mountain are excluded'. Scorer does not accept the methods used by the above authors as suitable 'special' second conditions, because the flow is unlikely to start from rest in nature, or to have a condition like a rigid lid, etc., and accordingly he writes (13) in the form

$$V\zeta_0 = C_1 \cos K^*z + D_1 \sin K^*z \quad (K^* = \pm \mathrm{i}K), \tag{19}$$

and takes the solution with $D_1 = 0$, since $\sin K^*z$ is zero at the ground. There is, of course, no disagreement when K is real, the form (15) being the only possible choice. Putting $D_1 = 0$ in (19) gives a sort of Cauchy principal value for the integral (although the singularities are branch points, not poles) and, as shown by Corby & Sawyer (1958*b*), this leads to waves both upstream and downstream, with equal amplitude. In a reply to Corby & Sawyer, Scorer (1958*b*) argues that trains of waves can be added or subtracted at will in order to cancel the upstream waves, and mathematically the solution will still be correct.

However, it seems to this author that adding on waves is simply equivalent to changing the boundary condition to the one used here, and that it is impossible to exclude simultaneously both upstream waves and terms which are zero at the ground.

The integral (17) will be evaluated in §3, with the condition described above, that the contour of the ξ-integral passes below the singularities.

The wave equation in case (*b*), with l^2 given by (8) is, from (5),

$$(V\zeta_0)'' - (V\zeta_0)\{k_1^2 - k^2L^2\,\mathrm{e}^{-2z/h}/\xi^2\} = 0, \tag{20}$$

where

$$k_1^2 = k^2 + q^2 = \xi^2 + \eta^2 + q^2. \tag{21}$$

To solve this we write

$$\Phi = khL\,\mathrm{e}^{-z/h}/|\xi|, \tag{22}$$

and take Φ as independent variable. Equation (20) then becomes

$$\Phi^2 \frac{\mathrm{d}^2}{\mathrm{d}\,\Phi^2}(V\zeta_0) + \Phi\frac{\mathrm{d}}{\mathrm{d}\Phi}(V\zeta_0) + (\Phi^2 - h^2k_1^2)(V\zeta_0) = 0, \tag{23}$$

which is Bessel's equation, with solutions $J_{hk_1}(\Phi)$, $Y_{hk_1}(\Phi)$. Since hk_1 is real and positive, and the solution is to be finite as $z \to \infty$ $(\Phi \to 0)$ we must write

$$V\zeta_0 = A_2 J_{hk_1}(hkL\,\mathrm{e}^{-z/h}/|\xi|). \tag{24}$$

We use the mountain shape (11) to determine the constant A_2, and so for case (*b*) we have

$$\zeta = \frac{Hab\,V(0)}{4\pi V(z)} \int_{-\infty}^{\infty}\int_{-\infty}^{\infty} \frac{\exp\{\mathrm{i}(\xi x + \eta y) - \frac{1}{4}a^2\xi^2 - \frac{1}{4}b^2\eta^2\} J_{hk_1}(hkL\,\mathrm{e}^{-z/h}/|\xi|)}{J_{hk_1}(hkL/|\xi|)}\,\mathrm{d}\xi\,\mathrm{d}\eta. \tag{25}$$

This integral is considered in §4, again with the condition that the path of the ξ-integral passes below the singularities.

3. The streamline displacement when l^2 is constant

This section is concerned with the double Fourier integral (17). In (17) we shall introduce non-dimensional variables with l^{-1} as unit of length and $V(0)$ as unit of velocity. Retaining the same symbols for the non-dimensional forms of the various quantities, we simply replace both l and $V(0)$ by unity.

At this stage we break away completely from the method of I by considering the ξ-integral first, and we approximate at once for large x $(x \gg 1)$. The main contribution to the integral then comes from the part of the contour near to the singularities of the integrand. In (17) we have branch points where

$$\{(\xi^2 - 1)(1 + \eta^2/\xi^2) + q^2\} = 0. \tag{26}$$

We can write (26) as

$$\xi^{-2}(\xi^2 - \xi_0^2)(\xi^2 + \xi_1^2) = 0, \tag{27}$$

giving branch points at $\xi = \pm\xi_0$, $\xi = \pm \mathrm{i}\xi_1$, with

$$\xi_0^2 = \tfrac{1}{2}[1 - q^2 - \eta^2 + \{(1 - q^2 - \eta^2)^2 + 4\eta^2\}^{\frac{1}{2}}], \tag{28}$$

and

$$\xi_1^2 = -\tfrac{1}{2}[1 - q^2 - \eta^2 - \{(1 - q^2 - \eta^2)^2 + 4\eta^2\}^{\frac{1}{2}}]. \tag{29}$$

When $q = 0$, $\xi_0 = 1$ (in the dimensional form $\xi_0 = l$) and $\xi_1 = \eta$. There is another branch point at theorigin. This arises from the change of sign of $\mathrm{i}\sqrt{(\xi_0^2 - \xi^2)}$ at the origin, as shown in (18) (where $\xi_0 = l$).

To work out the details, we deform the contour in the ξ-plane as shown in figure 1, so that it passes into the upper half-plane for $x > 0$ and into the lower half-plane for $x < 0$. The parts of the deformed contour which are parallel to the real axis are taken far enough away from the axis to ensure that the integrals along them give a negligible contribution to the total; the circular arcs at infinity also give no contribution. As was found in similar cases in I, the part of the path along the imaginary axis will give a non-wave term, ζ_N, which will appear whether $x > 0$ or $x < 0$. This will include the effect of the branch points at $\xi = \pm i\xi_1$. The non-wave part of the disturbance will not be discussed here; we shall consider simply the wave term, ζ_W, given by the loop integrals around $\xi = +\xi_0$ and $\xi = -\xi_0$, which only appears for $x > 0$ (downstream). To the same order of approximation the paths of these loop-integrals can be considered as coming from infinity along the broken lines in figure 1.

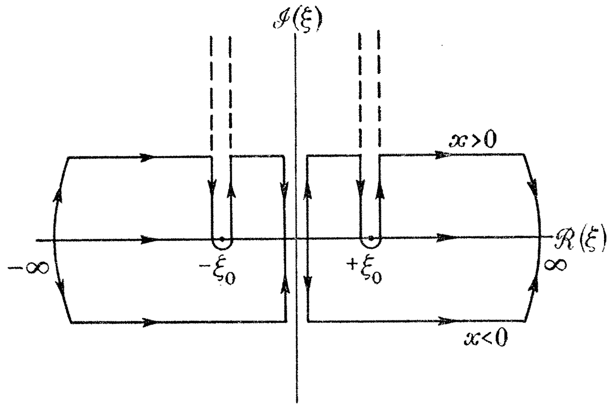

FIGURE 1. Contours of integration in the ξ-plane.

Taking first the right-hand loop we substitute

$$\xi = \xi_0 + i\psi^2, \tag{30}$$

so that, since x is assumed large, we shall be concerned only with small ψ. The ξ-integral in (17) becomes, on neglecting terms $O(\psi^3)$ and omitting all factors not depending on ξ,

$$\int_0^\infty \exp(i\xi_0 x - x\psi^2)\{\exp[-z\{(1+\xi_1^2/\xi_0^2)\,2\xi_0\psi\}^{\frac{1}{2}}\,e^{\frac{1}{4}i\pi}] - \exp[-z\{(1+\xi_1^2/\xi_0^2)\,2\xi_0\psi\}^{\frac{1}{2}}\,e^{-\frac{3}{4}i\pi}]\}$$
$$\times \exp(-\tfrac{1}{4}a^2\xi_0^2 - \tfrac{1}{2}ia^2\xi_0\psi^2)\,2i\psi\,d\psi. \tag{31}$$

This comes from the straight parts of the loops only. Certain terms in the powers of the exponentials in the large bracket which have third or higher powers of ψ and which also contain a factor involving η have been neglected. This would appear to be unjustifiable because η can become large. However, when η is large the integrand as a whole is small on account of the $e^{-\frac{1}{4}b^2\eta^2}$ factor (not shown in (31)) and therefore the approximation will be adequate. The approximation is adequate only if $z \ll x^{\frac{3}{4}}$, since otherwise the terms in $z\psi^3$ may be comparable with $x\psi^2$. The expression (31) can be written

$$2i\exp\left\{i\xi_0 x - \tfrac{1}{4}a^2\xi_0^2 + \frac{iz(\xi_0^2+\xi_1^2)}{2\xi_0(x+\frac{1}{2}ia^2\xi_0)}\right\}\int_{-\infty}^{\infty}\exp\left[-(x+\tfrac{1}{2}ia^2\xi_0)\left\{\psi + \frac{z\,e^{\frac{1}{4}i\pi}(\xi_0^2+\xi_1^2)^{\frac{1}{2}}}{(2\xi_0)^{\frac{1}{2}}(x+\frac{1}{2}ia^2\xi_0)}\right\}^2\right]\psi\,d\psi, \tag{32}$$

$$= \exp\left\{i\xi_0 x - \tfrac{1}{4}a^2\xi_0^2 + \frac{iz^2(\xi_0^2+\xi_1^2)}{2\xi_0(x+\frac{1}{2}ia^2\xi_0)} - \tfrac{1}{4}i\pi\right\}\frac{z\{2\pi(\xi_0^2+\xi_1^2)\}^{\frac{1}{2}}}{\xi_0^{\frac{1}{2}}(x+\frac{1}{2}ia^2\xi_0)^{\frac{3}{2}}}. \tag{33}$$

The left-hand loop integral is given similarly by substituting $\xi = -\xi_0 + i\psi^2$ and is equal to the complex conjugate of (33). From the two contributions we have

$$\zeta_W \sim \sum_{\pm} \frac{Habz\, e^{\mp\frac{1}{4}i\pi}}{2^{\frac{3}{2}}\pi^{\frac{1}{2}}V(z)\,x^{\frac{3}{2}}} \int_{-\infty}^{\infty} \exp\left\{\pm i\xi_0 x - \tfrac{1}{4}a^2\xi_0^2 + i\eta y - \tfrac{1}{4}b^2\eta^2 \pm \frac{iz^2(\xi_0^2+\xi_1^2)}{2\xi_0 x}\right\}\left\{\frac{\xi_0^2+\xi_1^2}{\xi_0}\right\}^{\frac{1}{2}} d\eta. \quad (34)$$

Here we have assumed $x \gg \frac{1}{2}a^2\xi_0$, to enable the factors $(x+\frac{1}{2}ia^2\xi_0)$ in (33) to be replaced by x. This is hardly a further restriction than $x \gg 1$ which is already assumed, unless a is too large; if a is large we expect from previous results that the waves will have very small amplitude.

We have now to evaluate the η-integral in (34). We shall first consider the case $q = 0$, and bring in non-zero q later. The case $q = 0$ has the advantage that we can work out the integral exactly in the special case of $y = 0$, giving the waves in the plane downstream of the peak of the mountain. With $q = 0$ and $y = 0$ the integral is

$$\int_{-\infty}^{\infty} e^{-B\eta^2}(1+\eta^2)^{\frac{1}{2}}\, d\eta, \quad (35)$$

where

$$B = \tfrac{1}{4}b^2 \mp iz^2/2x \quad (36)$$

and $|\arg B| < \frac{1}{2}\pi$. We have here used the fact that for $q = 0$, $\xi_0 = 1$ and $\xi_1 = \eta$. Substituting $\eta = \sinh\tau$, (35) becomes

$$\left(1 - \frac{d}{dB}\right)\int_{-\infty}^{\infty} e^{-B\sinh^2\tau}\, d\tau, \quad (37)$$

$$= \left(1 - \frac{d}{dB}\right) e^{\frac{1}{2}B} K_0(\tfrac{1}{2}B) \quad (38)$$

by Watson (1944, §6·22(7)), first writing $\sinh^2\tau$ in terms of $\cosh 2\tau$. Here K_0 is the Bessel function of imaginary argument.

Thus in the plane $y = 0$

$$\zeta_W \sim \sum_{\pm} \frac{Habz}{2^{\frac{5}{2}}\pi^{\frac{1}{2}}V(z)\,\rho^{\frac{1}{2}}(z)\,x^{\frac{3}{2}}} \exp\{\pm ix - \tfrac{1}{4}a^2 \pm iz^2/4x \mp \tfrac{1}{4}i\pi + \tfrac{1}{8}b^2\}$$
$$\times \{K_0(\tfrac{1}{8}b^2 \mp iz^2/4x) + K_1(\tfrac{1}{8}b^2 \mp iz^2/4x)\}, \quad (39)$$

$$= \frac{Habz\exp(-\frac{1}{4}a^2+\frac{1}{8}b^2)}{2^{\frac{3}{2}}\pi^{\frac{1}{2}}V(z)\,\rho^{\frac{1}{2}}(z)\,x^{\frac{3}{2}}}\mathscr{R}[\exp\{ix + iz^2/4x - \tfrac{1}{4}i\pi\}\{K_0(\tfrac{1}{8}b^2 - iz^2/4x) + K_1(\tfrac{1}{8}b^2 - iz^2/4x)\}], \quad (40)$$

when $x \gg \frac{1}{2}a^2\xi_0$, $z \ll x^{\frac{3}{4}}$, and $q = 0$. Here $\rho(z)$ is the non-dimensional density, taking $\rho(0)$ as unit; this factor was omitted after equation (6).

For the purpose of comparing this result with the results of I it is advantageous to consider separately the special cases of $xb^2 \gg 2z^2$ and $xb^2 \ll 2z^2$ for which (40) reduces to

$$\zeta_W \sim \frac{Habz\exp(-\frac{1}{4}a^2+\frac{1}{8}b^2)}{2^{\frac{3}{2}}\pi^{\frac{1}{2}}V(z)\,\rho^{\frac{1}{2}}(z)\,x^{\frac{3}{2}}}\cos(x - \tfrac{1}{4}\pi)\{K_0(\tfrac{1}{8}b^2) + K_1(\tfrac{1}{8}b^2)\}, \quad (41)$$

and

$$\zeta_W \sim \frac{Habz\, e^{-\frac{1}{4}a^2}}{2^{\frac{3}{2}}\pi^{\frac{1}{2}}V(z)\,\rho^{\frac{1}{2}}(z)\,x^{\frac{3}{2}}}\mathscr{R}[\exp\{ix + iz^2/4x - \tfrac{1}{4}i\pi\}\{K_0(-iz^2/4x) + K_1(-iz^2/4x)\}], \quad (42)$$

respectively. The form (41) gives the waves in the plane $y = 0$ at low levels for a mountain of small width perpendicular to the air stream (i.e. small b), but applies to larger heights for

PHILOSOPHICAL TRANSACTIONS OF THE ROYAL SOCIETY A MATHEMATICAL, PHYSICAL & ENGINEERING SCIENCES

wider mountains. The second form, (41), applies only to mountains with very small b, because our approximations are not valid if z is too large.

The restrictions on (41) are much the same as those on I(137), which in the plane $y = 0$ gave

$$\zeta_W \sim -\frac{2^{\frac{3}{2}} Haz}{\pi^{\frac{1}{2}} V(z)\, \rho^{\frac{1}{2}}(z)\, x^{\frac{3}{2}}} \cos\left(x+\tfrac{3}{4}\pi\right) \{K_1(a)+aK_0(a)\} + O\left(x^{-\frac{5}{2}}\right) \qquad \text{(I 137)}$$

for a circular mountain. Putting $b = a$ in (41) makes it very similar to (I 137), but we must allow for the fact that the mountains are not exactly the same shape.

However, with (41) we can see the variation of the amplitude of the waves as we increase b keeping a constant, so that the elliptical mountain eventually becomes an infinite ridge. This variation is shown in curve 1 of figure 2. It is clear that for values of b above about 5, say, the waves in the plane $y = 0$ for the elliptical mountain are almost identical with the waves in the lee of a ridge ($b = \infty$) which has the same height, H, and width in the x-direction, a. Moreover, for a mountain with b smaller than 5 (but still large enough for (41) to be suitable), the wave amplitude in the plane $y = 0$ is greater than the amplitude of waves in the lee of the ridge. This rather surprising result confirms what was found in I.

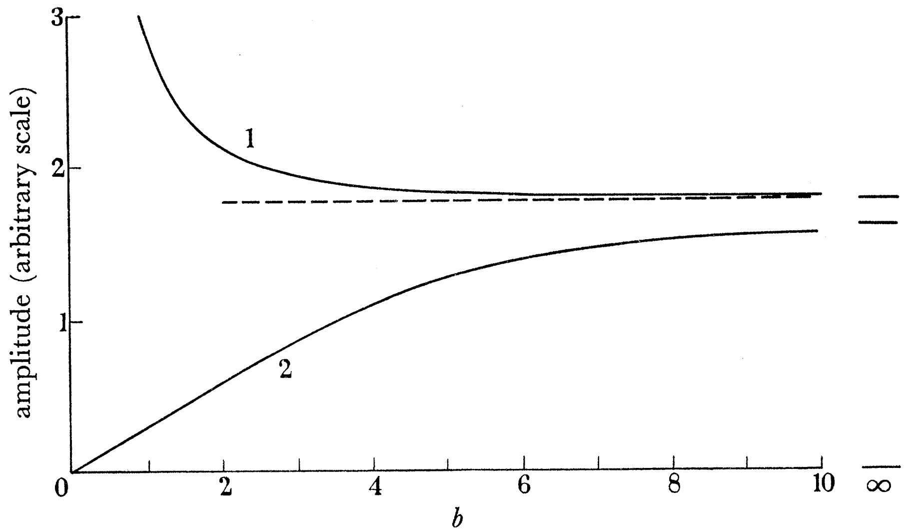

FIGURE 2. The amplitude of the waves in the plane $y = 0$ as a function of b, the parameter governing the width of the mountain perpendicular to the undisturbed air stream, when l^2 is constant. Curve 1 is for $q = 0$, $xb^2 \gg 2z^2$; curve 2 is for $q = 1/\sqrt{2}$, $a = \sqrt{2}$, $x = 5$, $z = \sqrt{10}$, and is accurate for b greater than about 5. The broken line showing amplitude independent of b is given by the approximation for $b > 5$, $xb^2 \gg 2z^2$ when $q = 0$. (a, b, x, z, q non-dimensional.)

When $xb^2 \ll 2z^2$, so that b is very small, and ζ_W takes the form (42), the wave disturbance is like that given by the 'doublet' solution in I; in fact, if we take a doublet strength $m = \pi Hab\, e^{-\frac{1}{4}a^2}$, (42) is identical with I (90) with $y = 0$. A very narrow mountain therefore gives behaviour like that given by doublet, a result in disagreement with the results of I. Finding this disagreement made necessary a re-examination of the earlier theory, which was found to be incorrect. The second (and dominant) singularity of the doublet case in I has in fact been found to exist in the circular mountain case, the error in proving that it did not arising through confusion of the directions of the cuts in the Riemann sheets of the

ξ-plane. However, for a circular mountain this singularity is no longer on the real axis (its distance from the axis depending on the mountain parameter a, which is zero for the doublet), and the waves to which it gives rise have an exponential decay with x. Because of this decay the waves can be shown to be negligible in all interesting cases, and the conclusions of I are unchanged. The corrected form of this section of I appears in Crapper (1959 *b*).

In order to obtain a solution which is valid for all y we will now apply the method of steepest descents (described in Watson 1944, §8·3) to the integral in (34). We shall retain the restriction $q = 0$. If some combination of y, $\frac{1}{4}b^2$ and $z^2/2x$ is large, the integral in (34) is dominated by the function

$$e^{f(\eta)} = \exp\left(i\eta y - \tfrac{1}{4}b^2\eta^2 \pm iz^2\eta^2/2x\right), \tag{43}$$

the other terms in the exponential being constants when $q = 0$. The integrand of (34) has a col where $f'(\eta) = 0$, i.e. at

$$\eta = \eta_0 = \frac{\mp 4xyz^2 + i2b^2x^2y}{b^4x^2 + 4z^4}, \tag{44}$$

and if the contour is suitably deformed to pass through η_0, the main contribution to the integral is from the part of the path near to this point. The required direction in which the path must pass over the col can be shown to make an angle $\pm\theta$ with the real axis, where

$$\theta = \tfrac{1}{2}\tan^{-1}(2z^2/b^2x) \quad (0 < \theta < \tfrac{1}{4}\pi) \tag{45}$$

(the signs corresponding with those of (43)), and the leading term of the approximation gives

$$\zeta_W \sim \frac{2^{\frac{1}{2}}Haz}{V(z)\,\rho^{\frac{1}{2}}(z)\,x^{\frac{3}{2}}}\left[\frac{b^4x^2\{(b^4x^2+4z^4)^2 + 8x^2y^2(-b^4x^2+4z^4+2x^2y^2)\}}{(b^4x^2+4z^4)^3}\right]^{\frac{1}{4}}$$
$$\times \exp\left\{-\tfrac{1}{4}a^2 - \frac{b^2x^2y^2}{(b^4x^2+4z^4)}\right\}\cos\left\{x + \frac{z^2}{2x} - \frac{2xy^2z^2}{b^4x^2+4z^4} - \tfrac{1}{4}\pi + \theta - \phi\right\}, \tag{46}$$

where
$$\phi = \tfrac{1}{2}\tan^{-1}\left\{\frac{16b^2x^3y^2z^2}{(b^4x^2+4z^4)^2 + 4x^2y^2(4z^4-b^4x^2)}\right\}. \tag{47}$$

In (46) we have carried out the summation over the $\pm$ signs from the two loop-integrals. This result (46) is subject to a further restriction which arises because the original η-integral (34) has branch points at $\eta = \pm i$ (when $q = 0$). These branch points make (46) incorrect if the col at $\eta = \eta_0$ is in such a position that the deformed contour of integration cuts the imaginary axis at a point with $|\eta| \geqslant i$. This means that we must have $y < \frac{1}{2}b^2$ for small values of $2z^2/b^2x$, with larger values of y allowable for larger $2z^2/b^2x$.

An approximation for large y (with $q = 0$) can be found by treating (34) as a loop integral around a branch point, the method being very similar to that already used for the ξ-integral. This gives

$$\zeta_W \sim \frac{2^{\frac{5}{4}}Haz}{V(z)\,\rho^{\frac{1}{2}}(z)\,x^{\frac{3}{2}}}\left[\frac{b^4x^6}{\{(2|y|-b^2)^2x^2+4z^4\}^3}\right]^{\frac{1}{4}}\exp\left(-\tfrac{1}{4}a^2 - |y| + \tfrac{1}{4}b^2\right)\cos\left(x + \tfrac{3}{4}\pi - \theta_1\right), \tag{48}$$

where
$$\theta_1 = \tfrac{3}{2}\tan^{-1}\left\{\frac{2z^2}{x(2|y|-b^2)}\right\}, \tag{49}$$

a result which does not differ from (46) in important features.

In the plane $y = 0$ the dependence on b of the amplitude of (46) is given by the factor $\{b^4x^2/(b^4x^2+4z^4)\}^{\frac{1}{4}}$. If we approximate for $xb^2 \gg 2z^2$, as we did previously in connexion with (40), this factor becomes unity, the parameter b then having disappeared from the result. This again shows that when b is large enough the waves in the plane $y = 0$ are exactly the same as the waves in the lee of the corresponding infinite ridge. In view of curve 1 of figure 2, this approximation, which is shown in figure 2 by the broken line, will be valid for $b > 5$, say. The full result (46) will be valid for slightly smaller values of b, since even when $y = 0$ (46) only requires $|\frac{1}{8}b^2 - \mathrm{i}z^2/4x|$ to be large. This can be seen by replacing the Bessel functions of the more exact result (40) by their asymptotic forms for large argument, which gives (46) with $y = 0$.

The remaining features of (46) and (48) confirm the results of I. As $|y|$ is increased the wave amplitude falls off rapidly, following the shape of the mountain, so that the waves are effectively contained in a strip behind the highest part of the mountain; increasing the width b simply increases the width of the strip. The rate of decay of amplitude downstream is as $x^{-\frac{3}{4}}$, and the amplitude increases more or less linearly with height z. These waves appear to be unlike other waves caused by three-dimensional disturbances, and to be in some ways two-dimensional in character.

To deal with the case of non-zero q we can use the same method of steepest descents, but a really satisfactory result can only be obtained for the waves in the plane $y = 0$. When $q \neq 0$ the previous $f(\eta)$ is replaced by

$$f(\eta) = \pm\mathrm{i}\xi_0 x - \tfrac{1}{4}a^2\xi_0^2 + \mathrm{i}\eta y - \tfrac{1}{4}b^2\eta^2 \pm \mathrm{i}z^2(\xi_0^2+\xi_1^2)/2x\xi_0, \tag{50}$$

since ξ_0 and ξ_1 now depend upon η, and

$$f'(\eta) = \pm\mathrm{i}\xi_0' x - \tfrac{1}{2}a^2\xi_0\xi_0' + \mathrm{i}y - \tfrac{1}{2}b^2\eta^2 \pm \frac{\mathrm{i}z^2}{2x}\left\{\xi_0' + 2\frac{\xi_1\xi_1'}{\xi_0} - \frac{\xi_0'\xi_1^2}{\xi_0^2}\right\}. \tag{51}$$

We need the value of η for which $f'(\eta) = 0$; when $y = 0$ this value is $\eta = 0$, because from (28) and (29) we can see that both ξ_0' and ξ_1 are zero at $\eta = 0$. Hence for $y = 0$ the steepest descents approximation gives

$$\zeta_W \sim \frac{Habz(1-q^2)^{\frac{1}{4}}\exp\{-\frac{1}{4}a^2(1-q^2)\}}{V(z)\,\rho^{\frac{1}{2}}(z)\,x^{\frac{3}{4}}\,C^{\frac{1}{2}}}\cos\{x(1-q^2)^{\frac{1}{2}} + z^2(1-q^2)^{\frac{1}{2}}/2x + \theta - \tfrac{1}{4}\pi\}, \tag{52}$$

where now
$$\theta = \tfrac{1}{2}\tan^{-1}\left\{\frac{2q^2x^2+(2+q^2)\,z^2}{a^2q^2(1-q^2)^{\frac{1}{2}}\,x + b^2(1-q^2)^{\frac{3}{2}}\,x}\right\}, \tag{53}$$

and
$$C = \left[\left\{\frac{a^2q^2}{2(1-q^2)} + \tfrac{1}{2}b^2\right\}^2 + \left\{\frac{q^2x}{(1-q^2)^{\frac{3}{2}}} + \frac{(2+q^2)\,z^2}{2(1-q^2)^{\frac{3}{2}}\,x}\right\}^2\right]^{\frac{1}{2}}. \tag{54}$$

When $q = 0$ (52) reduces to the previous steepest descents result (46), with $y = 0$. Equation (46) was subject to the restriction that $|\frac{1}{8}b^2 - \mathrm{i}z^2/4x|$ must be large ($y = 0$), and it follows that this must also apply to (52), at least when q is small, even though $f(\eta)$ now contains a term in x. We can also see from (52) that if q^2 is near to unity the wave-length, which is approximately $2\pi/(1-q^2)^{\frac{1}{2}}$, becomes very large. The reason for this is that the branch points in the ξ-plane are in this case close to the origin, and thus the wave terms and non-wave terms should not be considered separately. We must therefore assume

$x(1-q^2)^{\frac{1}{2}} \gg 1$ in (52), in addition to the restriction $|\frac{1}{8}b^2 - iz^2/4x| \gg 1$ and our previous assumptions of $x \gg \frac{1}{2}a^2\xi_0$ ($x \gg \frac{1}{2}a^2(1-q^2)^{\frac{1}{2}}$ in (52)) and $z \ll x^{\frac{3}{4}}$. If q^2 is actually greater than unity the branch points move on to the imaginary ξ axis when $\eta = 0$, and we have definitely no waves in the plane $y = 0$.

The introduction of non-zero q has changed the form of the waves considerably. They now decay downstream as $x^{-\frac{3}{2}}$ if b is finite, although the decay is still as $x^{-\frac{1}{2}}$ for the infinite ridge. The behaviour of the amplitude as a function of b is also changed. As b increases the amplitude increases, and eventually tends to the value given by the infinite ridge. This is shown for a particular case in curve 2 of figure 2; smaller values of q than that shown ($q = 1/\surd 2$) make the amplitude tend to its limiting value more rapidly. The striking difference between curves 1 and 2 of figure 2 is of course that in curve 1 ($q = 0$) the amplitude is greater for finite b than for the ridge, whereas in curve 2 it is less.

When neither y nor q is zero the problem can only be solved for a 'doublet' type of disturbance which we get by assuming that both a and b are small. The integrand of (34) is then dominated by

$$e^{f(\eta)} = \exp(\pm i\xi_0 x + i\eta y), \tag{55}$$

and we can approximate to the integral by the method of stationary phase. This approach is dealt with in detail in § 4, below, when considering the case of exponential l^2. The results of this method depend on the shape of the curve of $\xi_0(\eta)$ against η; a particular example of this is shown in figure 3. This curve has roughly the same shape as the curves used in § 4, and we shall see that it will lead to waves which are contained in a wedge downstream of the mountain, resembling ship waves. However, it is not worth giving the details of the solution in this section as the method breaks down in the most interesting case, when q is small. We can see this by considering the solution for $y = 0$: in the doublet solution the $C^{\frac{1}{2}}$ of (52) is replaced by $\{q^2x/(1-q^2)^{\frac{3}{2}}\}^{\frac{1}{2}}$, but when q is small this term is at most of only the same order as the other terms in $C^{\frac{1}{2}}$.

4. The streamline displacement when l^2 falls off exponentially with height

We now turn our attention to the integral (25). Again we shall introduce non-dimensional variables, this time taking h as unit of length, and keeping $V(0)$ as unit of velocity. Again retaining the same symbols for the non-dimensional forms of the various quantities, we simply replace both h and $V(0)$ by unity.

The integral (25) is different from (17), discussed in § 3, because in general the integrand has poles, where

$$J_{\surd(\xi^2+\eta^2+q^2)}\left\{\frac{\surd(\xi^2+\eta^2)\,L}{|\xi|}\right\} = 0. \tag{56}$$

Even so, the general approach applied in § 3 can be used here.

Considering, then, the ξ-integral first we again deform the contour as in figure 1, into the upper half-plane for $x > 0$ and into the lower half-plane for $x < 0$, but we can omit the loops around $\xi = \pm\xi_0$ as we now have no branch points. Here the ξ-integral is equal to the sum of the residues at poles inside the half-plane considered, poles on the real axis being regarded as in the upper half-plane, to give waves downstream, *plus* the contribution from the integrals along the imaginary axis and round the origin. The other parts of the contour give no contribution, as before. The loop around the origin will give a non-wave term and will not be discussed here. The values of L and q will determine the position of the poles, which give waves; for some L and q there may be no poles, and hence no waves.

If (49) has solutions $\xi = \xi_n(\eta)$, for $n = 1, 2, 3, \ldots$, where some of the ξ_n may be complex, then

$$\zeta_W = \frac{Hab}{4\pi V(z)} \int_{-\infty}^{\infty} \exp\left(\mathrm{i}\eta y - \tfrac{1}{4}b^2\eta^2\right) \sum_n \left[\frac{2\pi \mathrm{i} J_{k_1}(kL\mathrm{e}^{-z}/|\xi|)\exp\left(\mathrm{i}\xi x - \tfrac{1}{4}a^2\xi^2\right)}{\partial\{J_{k_1}(kL/|\xi|)\}/\partial\xi}\right]_{\xi=\xi_n(\eta)} \mathrm{d}\eta. \quad (57)$$

The real values of $\xi_n(\eta)$ can be found from tables of zeros of Bessel functions; the real zeros of $J_\nu(Z)$ are shown in figure 4. Only one quadrant of the $\nu - Z$ plane is shown because in (56) $\nu \geq q \geq 0$ and $Z \geq L \geq 0$. Graphs of $\xi_n(\eta)$ from poles on the real axis are shown in figures 5, 6 and 7 for various values of L, with $q = 0$, and figure 6 shows the effect of non-zero q. The significance of the various values of L will be seen later. Curves from zeros of (56) of higher order than those shown pass through the origin, and have been omitted. It should be noted also that these curves are symmetrical about both axes, and only one quadrant is shown. This implies that there are two poles for each value of η, at $\xi = \pm|\xi_n(\eta)|$.

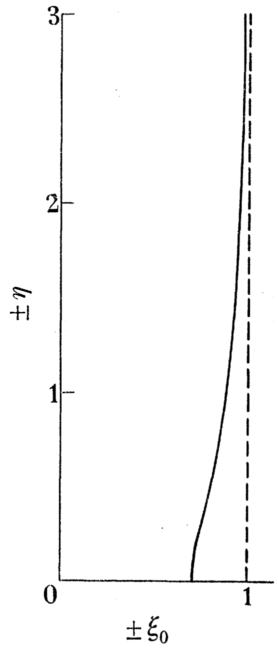

FIGURE 3. The function $\xi_0(\eta)$ when $q = 1/\sqrt{2}$ (q non-dimensional). The curve is symmetrical about both axes, only one quadrant being shown. When $q = 0$ we get the broken line, $\xi_0 = 1$.

It would seem likely that there will also be some poles which are not on the real axis of the ξ-plane, and indeed, such poles do appear in some of the two-dimensional numerical solutions of Sawyer (1960), giving significant contributions to the integral. The waves due to these poles decay exponentially with increase of x, so that only poles which are near to the real axis are important. The exponential factor must be a decay, not an increase, because of the fact that we have to deform the contour into the upper or lower half-planes according as $x > 0$ or $x < 0$. There does not seem to be any reason why poles at complex values of ξ should not appear in the lower half-plane, leading to upstream waves with an exponential decay, although in considering various air streams, all the poles found by Sawyer (1960) were on or above the real axis. However, Sawyer was unable to prove that this would always be the case.

In the present problem we can definitely say that there are no poles at complex values of ξ in one special case, when $\eta = 0$. In this case the argument of the Bessel function in (56) is real ($= L$), although the order ($= \sqrt{(\xi^2+q^2)}$) will be complex if ξ is complex. Beckmann & Franz (1957) show the curve in the ν-plane on which the zeros of $J_\nu(Z)$ lie ($J_\nu(\rho)$ in their notation; the curve is marked j in their figure 13). When Z is real this curve lies along the real ν axis. Thus the only poles when $\eta = 0$ must be for real $\sqrt{(\xi^2+q^2)}$, i.e. for real ξ. (Any poles for pure imaginary ξ, for which $\sqrt{(\xi^2+q^2)}$ could still be real, will contribute only to the non-wave term.) We shall see that the waves in the plane $y = 0$, immediately downstream of the mountain peak, depend on the case $\eta = 0$, and thus all these waves come from

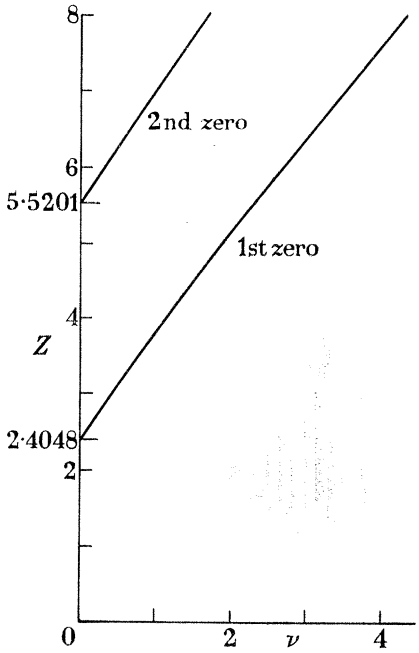

FIGURE 4. Zeros of $J_\nu(Z)$ for real and positive ν and Z.

poles on the real axis. This suggests that even if poles exist at complex values of ξ when $\eta \neq 0$, their contribution to the integral is not likely to be significant. As the author is at present unable even to establish the existence of such poles, they will not be considered further here.

To complete the solution for the wave terms arising from poles on the real axis we have to evaluate the integral (57), with $\xi_n(\eta)$ real when η is real. The best approach still seems to be to approximate by the method of steepest descents, although here again the method is too difficult to give us a satisfactory answer in the general case. For a particular n, and when x is large, the integral is dominated by the factor

$$e^{f(\eta)} = \exp\left(i\xi_n(\eta)\,x + i\eta y - \tfrac{1}{4}a^2\xi_n^2(\eta) - \tfrac{1}{4}b^2\eta^2\right), \tag{58}$$

and

$$f'(\eta) = i\xi_n'(\eta)\,x + iy - \tfrac{1}{2}a^2\xi_n(\eta)\,\xi_n'(\eta) - \tfrac{1}{2}b^2\eta. \tag{59}$$

In general the cols, at points where $f'(\eta) = 0$ will be at complex values of η, with corresponding complex values of $\xi_n(\eta)$. Because of the complicated nature of $\xi_n(\eta)$ we cannot write

PHILOSOPHICAL TRANSACTIONS OF THE ROYAL SOCIETY A MATHEMATICAL, PHYSICAL & ENGINEERING SCIENCES

down the general positions of the cols, and we can only deal with two special cases. These are cases already used for non-zero q in §3, namely, the waves in the plane $y = 0$ and a 'doublet' solution.

When $y = 0$ we again have a col at $\eta = 0$. To see this we first differentiate (56) with respect to η, in order to examine $\xi_n'(\eta)$:

$$\frac{\partial J_\nu(Z)}{\partial Z}\left\{\frac{\eta\xi_n-\eta^2\xi_n'}{\xi_n|\xi_n|\sqrt{(\xi_n^2+\eta^2)}}\right\}L+\frac{\partial J_\nu(Z)}{\partial \nu}\left\{\frac{\xi_n\xi_n'+\eta}{\sqrt{(\xi_n^2+\eta^2+q^2)}}\right\}=0, \tag{60}$$

with

$$\nu=\sqrt{(\xi_n^2+\eta^2+q^2)} \tag{61}$$

and

$$Z=\frac{\sqrt{(\xi_n^2+\eta^2)}\,L}{|\xi_n|}. \tag{62}$$

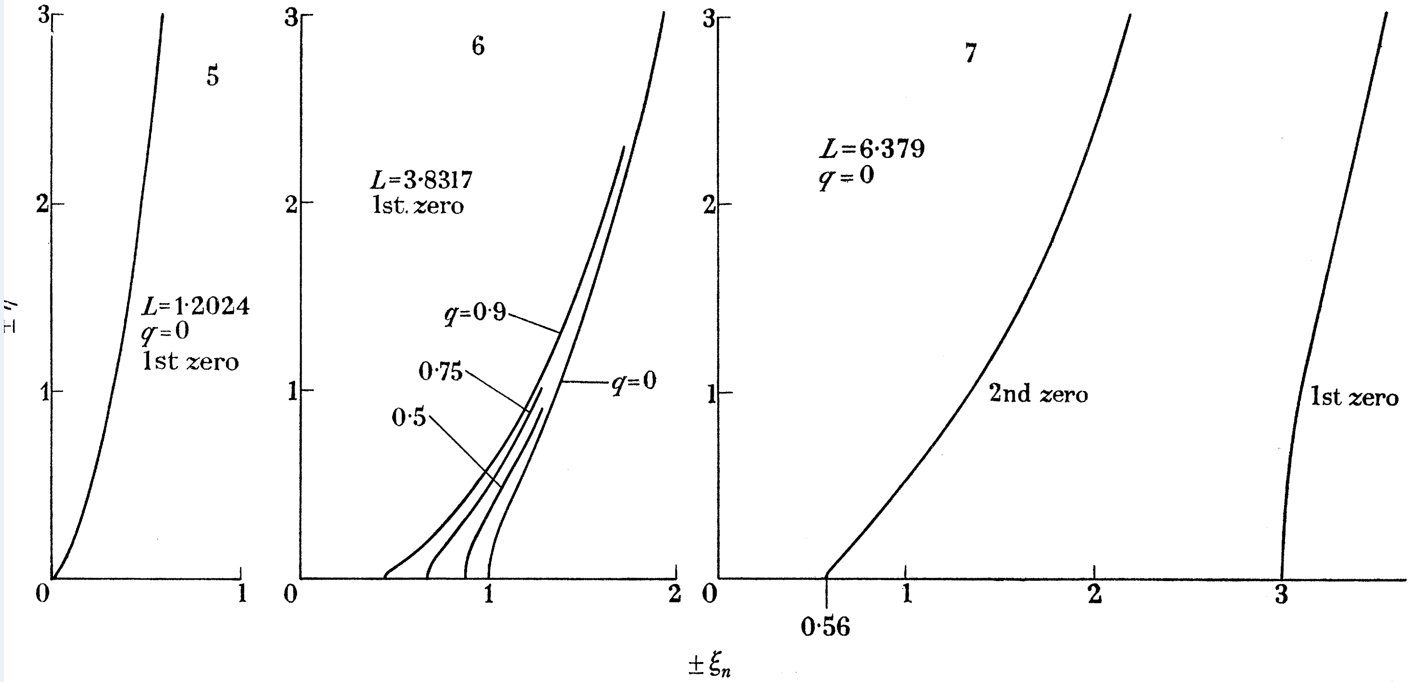

FIGURES 5, 6 AND 7. The function $\xi_n(\eta)$ for $L = 1{\cdot}2024$, $q = 0$ (figure 5); $L = 3{\cdot}8317$, $q = 0$, $0{\cdot}5$, $0{\cdot}75$, $0{\cdot}9$ (figure 6); $L = 6{\cdot}379$, $q = 0$ (figure 7) (L and q non-dimensional). All the curves are symmetrical about both axes, only one quadrant being shown in each case. The curves come from the first or second real zero of the Bessel function (56) as indicated; all curves from real zeros of higher order than those shown in any particular figure resemble the curve of figure 5, passing through the origin. In figure 6 the curve from the first zero passes through the origin when $q = 1$.

For (60) to be satisfied at $\eta = 0$ either $\xi_n(0)$ or $\xi_n'(0)$ must normally be zero. This fact is illustrated in figures 5 to 7: in figure 5 $\xi_n(0) = 0$ and in figures 6 and 7 $\xi_n'(0) = 0$. However, we shall see that the wavelength of the waves in the plane $y = 0$, λ, is approximately $2\pi/\xi_n(0)$, so that when $\xi_n(0) = 0$ we have infinite wavelength—i.e. all the disturbance belongs to the non-wave term which we are not considering here. Thus for wave terms to appear L and q must be such that $\xi_n'(0) = 0$. Hence, from (59) there is a col at $\eta = 0$ when $y = 0$.

The ranges of L and q which determine the existence of waves in the plane $y = 0$ thus depend on the zeros of the Bessel function (56) with $\eta = 0$—i.e. the zeros of $J_\nu(Z)$ (figure 4) with $\nu = \surd(\xi_n^2(0)+q^2)$ and $Z = L$. Taking $q = 0$, so that $\nu = |\xi_n(0)|$, we see from figure 4 that if $L \leqslant 2{\cdot}4048$ there is apparently no value of $\xi_n(0)$ corresponding to a zero of the Bessel function; if $2{\cdot}4048 < L \leqslant 5{\cdot}5201$ there is one non-zero value of $\xi_n(0)$ corresponding to a zero; if $5{\cdot}5201 < L \leqslant 8{\cdot}6537$ (upper limit not shown) there are two non-zero values of $\xi_n(0)$, and so on. If q is increased these limiting values are increased. Values of L from each of the first three ranges were chosen in drawing figures 5 to 7. It is clear from figure 5 that when $L < 2{\cdot}4048$, $\xi_n(0) = 0$ corresponds to a pole from the first zero of the Bessel function. This is the limiting value of $\xi_n(\eta)$ as $\eta \to 0$. Curves from higher-order zeros than those shown in figures 5 to 7 also have $\xi_n(0) = 0$, and thus do not correspond to waves. To get a non-zero value of $\xi_n(0)$, and hence to get waves, we therefore need $L > 2{\cdot}4048$ (L non-dimensional). This agrees with Scorer's result (1949) for two-dimensional lee waves when l^2 is equal to different constants in different layers of the atmosphere, that to get poles, and the corresponding waves, l^2 must decrease sufficiently rapidly with height.

For values of L near to the limiting values the wavelength will be very long and the disturbance will not be of any interest as waves. Moreover, in these cases, the contribution from the pole will be affected by the branch point at the origin, as the two singularities will be close together, and would have to be considered together for an accurate result. We will therefore exclude values of L and q for which $\xi_n(0) \ll 1$, and take only true wave terms.

The direction of integration over the col at $\eta = 0$ is again easily shown to be

$$\pm\theta = \pm\tfrac{1}{2}\tan^{-1}\left\{\frac{2\xi_n'' x}{a^2\xi_n\xi_n''+b^2}\right\} \quad (0<\theta<\tfrac{1}{4}\pi), \tag{63}$$

where $\xi_n = |\xi_n(0)|$ and $\xi_n'' = |\xi_n''(0)|$. The $\pm$ signs correspond to the two poles which exist for one value of η, at $\xi = \pm\xi_n$. In writing down the wave term we can now add together the two values given by the $\pm$ signs for each n, but we must restrict our values of n to the number of positive roots ξ_n of (56). The first term of the steepest descents approximation then gives in the plane $y = 0$, for $x \gg 1$,

$$\zeta_W \sim \sum_{\pm}\sum_{n} \frac{Hab}{4\pi V(z)} \frac{2\pi \mathrm{i} J_{\surd(\xi_n^2+q^2)}(L\mathrm{e}^{-z})}{\left\{\pm\dfrac{\partial}{\partial|\xi|}J_{k_1}\left(\dfrac{kL}{|\xi|}\right)\right\}_{|\xi|=\xi_n,\,\eta=0}} \frac{(2\pi)^{\frac{1}{2}}\exp(\pm\mathrm{i}\xi_n x-\frac{1}{4}a^2\xi_n^2\pm\mathrm{i}\theta)}{C^{\frac{1}{2}}}, \tag{64}$$

where now
$$C = (\tfrac{1}{4}a^2\xi_n^2\xi_n''^2+\tfrac{1}{4}b^2+\tfrac{1}{2}a^2b^2\xi_n\xi_n''+\xi_n''^2x^2)^{\frac{1}{2}}. \tag{65}$$

Equation (64) simplifies to give

$$\zeta_W \sim -\sum_{n} \frac{Hab(2\pi)^{\frac{1}{2}}J_{\surd(\xi_n^2+q^2)}(L\mathrm{e}^{-z})\,\mathrm{e}^{-\frac{1}{4}a^2\xi_n^2}\surd(\xi_n^2+q^2)\sin(\xi_n x+\theta)}{V(z)\,\rho^{\frac{1}{2}}(z)\,\{\partial J_\nu(L)/\partial\nu\}_{\nu=\surd(\xi_n^2+q^2)}\,\xi_n C^{\frac{1}{2}}}. \tag{66}$$

Again we have re-introduced the non-dimensional density term $\rho^{\frac{1}{2}}(z)$ omitted after (6).

The second special case, the 'doublet' solution again applies only to waves in the lee of small mountains, with a and b each small compared with $\surd(x^2+y^2)$. With this condition the integral in (57) is dominated by

$$\mathrm{e}^{f(\eta)} = \exp(\mathrm{i}\xi_n(\eta)x+\mathrm{i}\eta y) \tag{67}$$

instead of (58). We can now use the method of Lighthill (1960) directly, although as we have only a double Fourier integral, compared with Lighthill's triple integral, we shall not find it necessary to rotate axes as Lighthill does.

From (67)
$$f'(\eta) = i\xi_n'(\eta)x + iy, \tag{68}$$
and $f'(\eta) = 0$ if
$$\xi_n'(\eta) = -y/x. \tag{69}$$

Equation (69) shows that $f'(\eta) = 0$ where the normal to the curve $\xi_n(\eta)$ is in the direction of the vector $\mathbf{r} = (x, y)$ (with the x and y axes coinciding with the ξ and η axes, respectively).

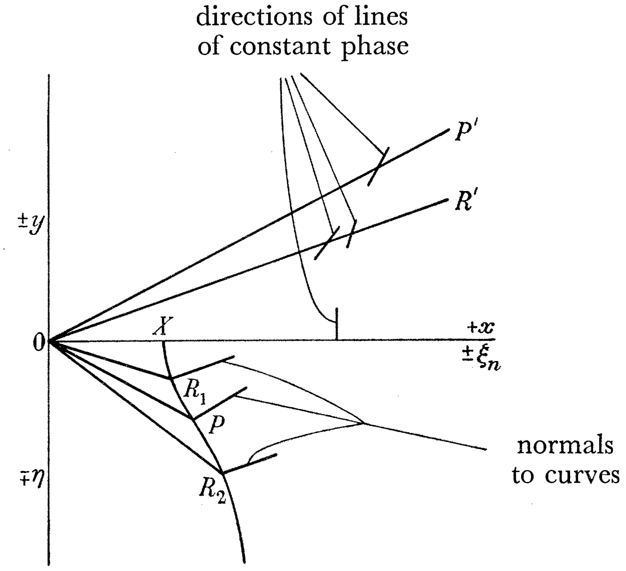

FIGURE 8. Construction of the lines of constant phase for the doublet solution. The upper half of the diagram represents the physical x–y plane, and the lower half represents the ξ–η plane. The curve $\xi = \xi_n(\eta)$ has a point of inflexion at P. Here the normal to the curve is parallel to OP', and therefore for points on OP' the col is at P, and the lines of constant phase are perpendicular to the wave-number vector **OP**. The normals at R_1 and R_2 are both parallel to OR', giving two cols and two sets of lines of constant phase at points on OR', one set perpendicular to $\mathbf{OR}_1$, the other perpendicular to $\mathbf{OR}_2$. Along OX the lines of constant phase are simply perpendicular to OX, the second set of waves having zero wavelength because the second normal parallel to OX is at $\eta = \pm\infty$. There are no waves outside the wedge with semi-angle $P'OX = \epsilon_m$, because there are no normals to $\xi = \xi_n(\eta)$ making angles $> \epsilon_m$ with OX.

The position of the col for a given $\mathbf{r}$ is thus completely determined by the geometry of the curve $\xi = \xi_n(\eta)$. Moreover, the final wave term will contain a factor
$$\exp(i\xi_n(\eta_n)\,x + i\eta_n y) = \exp(i\mathbf{k}_n.\mathbf{r}),$$
where $\mathbf{k}_n = (\xi_n(\eta_n), \eta_n)$, η_n being the value at the col. Therefore $\mathbf{k}_n$ is the wave number vector for the particular x, y chosen and the wave crests will be perpendicular to $\mathbf{k}_n$. This enables us to sketch the lines of constant phase quite simply; the method is demonstrated graphically in figure 8. The resulting lines are exactly like those of ship waves.

The curve $\xi = \xi_n(\eta)$ has points of inflexion (in the cases which give waves, e.g. figures 6 and 7) and at these points the normals to the curve make certain angles, $\pm\epsilon_m(\epsilon_m > 0)$, say, with the x axis. The normals at all other points of the curve make angles ϵ, where $|\epsilon| < \epsilon_m$, with the x axis. There are thus no cols, and hence no waves for directions of $\mathbf{r}$ with

$|\tan^{-1}(y/x)| = |\epsilon| > \epsilon_m$; for directions of $\mathbf{r}$ with $|\epsilon| < \epsilon_m$ there are two normals parallel to $\mathbf{r}$, and hence two cols, which give us two sets of waves, corresponding to the 'diverging' and 'transverse' sets of ship waves. This wave pattern is in agreement with the result of Scorer & Wilkinson (1956) for an air-stream with l^2 constant in layers.

The zeros of (56) which give curves with $\xi_n(0)$ zero or almost zero will again lead to very long waves, and will not be dealt with here. It will be clear, however, that only the waves in the plane $y = 0$ will have a strictly infinite wavelength when the curve $\xi = \xi_n(\eta)$ is of the type shown in figure 5.

Having determined η_n for the particular x, y being considered we can write down ζ_W by the method of stationary phase as $f(\eta)$ is entirely imaginary. This gives for $x \gg 1$, $\surd(x^2+y^2) \gg a, b$,

$$\zeta_W \sim \sum_{\pm}\sum_n \frac{Hab}{4\pi V(z)\,\rho^{\frac{1}{2}}(z)} \exp\left(\pm i\xi_{nn}x \pm i\eta_n y - \tfrac{1}{4}a^2\xi_{nn}^2 - \tfrac{1}{4}b^2\eta_n^2 \pm \tfrac{1}{4}i\pi\,\mathrm{sgn}\,\xi''_{nn}\right) \times \left\{\frac{2\pi}{|\xi''_{nn}|\,x}\right\}^{\frac{1}{2}} \left\{\frac{2\pi i\,J_{k_1}(kL\,e^{-z}/|\xi|)}{\pm\dfrac{\partial}{\partial|\xi|}J_{k_1}\left(\dfrac{kL}{|\xi|}\right)}\right\}_{\xi=\xi_{nn},\,\eta=\eta_n}, \tag{70}$$

where η_n is now the value of η at the col which corresponds to a positive value of $\xi_n(\eta)$ (η_n will be $\gtrless 0$ if $y \lessgtr 0$, from figure 8), $\xi_{nn} = \xi_n(\eta_n) > 0$ and $\xi''_{nn} = \xi''_n(\eta_n)$. The function $\mathrm{sgn}\,\xi''_{nn}$ equals ± 1 according as $\xi''_{nn} \gtrless 0$. The $\pm$ signs in (70) are again due to the fact that the part of the curve $\xi = \xi_n(\eta)$ with ξ negative gives a contribution to the downstream wave. On being rearranged, (70) becomes

$$\zeta_W \sim -\sum_n \frac{Hab(2\pi)^{\frac{1}{2}}}{V(z)\,\rho^{\frac{1}{2}}(z)} \left\{\frac{J_{k_1}(kL\,e^{-z}/|\xi|)}{\dfrac{\partial}{\partial|\xi|}J_{k_1}\left(\dfrac{kL}{|\xi|}\right)}\right\}_{\xi=\xi_{nn},\,\eta=\eta_n} \times \frac{\exp\left(-\tfrac{1}{4}a^2\xi_{nn}^2 - \tfrac{1}{4}b^2\eta_n^2\right)}{(|\xi''_{nn}|\,x)^{\frac{1}{2}}} \sin\left(\xi_{nn}x + \eta_n y + \tfrac{1}{4}\pi\,\mathrm{sgn}\,\xi''_{nn}\right) \tag{71}$$

(+ possible wave terms from poles not on the real axis of the ξ-plane ($\eta_n \neq 0$)).

This form of solution breaks down if ξ_{nn}, η_n are near to the points of inflexion, because there $\xi''_{nn} = 0$. If x, y actually correspond to a point of inflexion, (71) is replaced by

$$\zeta_W \sim -\sum_n \frac{Hab\,\Gamma(\frac{1}{3})\,6^{\frac{1}{3}}}{V(z)\rho^{\frac{1}{2}}(z)\,3^{\frac{1}{2}}} \left\{\frac{J_{k_1}(kL\,e^{-z}/|\xi|)}{\dfrac{\partial}{\partial|\xi|}J_{k_1}\left(\dfrac{kL}{|\xi|}\right)}\right\}_{\xi=\xi_{nn},\,\eta=\eta_n} \frac{\exp\left(-\tfrac{1}{4}a^2\xi_{nn}^2 - \tfrac{1}{4}b^2\eta_n^2\right)}{(|\xi'''_{nn}|x)^{\frac{1}{3}}} \sin(\xi_{nn}x + \eta_n y). \tag{72}$$

Thus exactly as with ship waves the rate of decay of amplitude is as $x^{-\frac{1}{2}}$ except near to the edges of the wedge, where it is as $x^{-\frac{1}{3}}$. It would therefore appear that the waves will be detectable further downstream near to the edges of the wedge. However, because of the factor $\exp(-\frac{1}{4}a^2\xi_{nn}^2 - \frac{1}{4}b^2\eta_n^2)$, and the fact that ξ_{nn} and η_n are smallest when $y = 0$, it is likely that only the waves which are roughly perpendicular to the air stream (the transverse system) will be large.

This doublet solution will apply to any elliptical mountain with finite a and b provided that x and y are taken large enough, but we can no longer let $b \to \infty$ and expect to get the infinite ridge solution. In fact as b increases the amplitude tends rapidly to zero. The full solution (66) for $y = 0$ gives a more reasonable result: as $b \to \infty$, $b/C^{\frac{1}{2}} \to \surd 2$, and the waves become like the two-dimensional waves of Palm & Foldvik (1960), with no decay downstream. The behaviour of the amplitude of (66) as a function of b is shown in figure 9, for various combinations of a and x. The amplitude approaches that of two-dimensional waves quite rapidly, although, as is to be expected, increase of either a or x increases the three-dimensional effect. For finite b the wave amplitude is smaller than the amplitude of waves in the lee of the infinite ridge; the value of q has no significant effect. This may be contrasted with the behaviour of the waves produced when l^2 is constant (figure 2). The curves of figure 9 are in fact very similar to curve 2 of figure 2, which applies when $q \neq 0$.

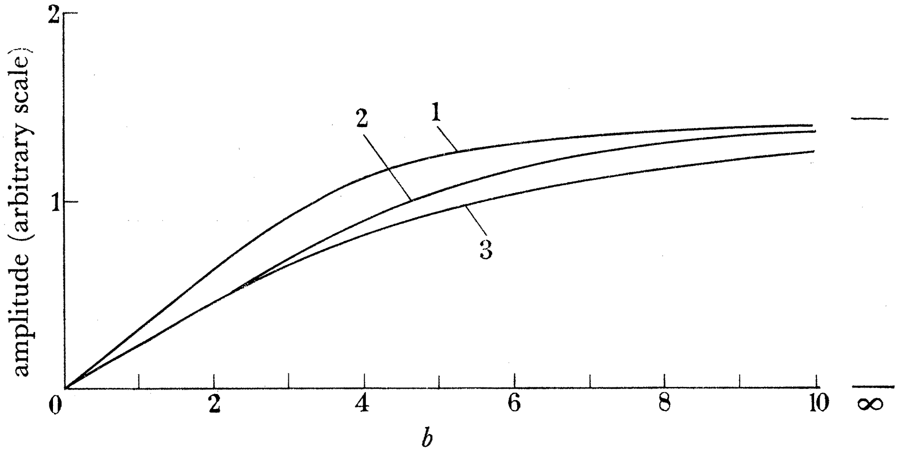

FIGURE 9. The amplitude of the waves in the plane $y = 0$ as a function of b, the parameter governing the width of the mountain perpendicular to the undisturbed air stream, when l^2 is exponential. In curve 1, $a = \sqrt{2}$, $x = 5$; in curve 2, $a = \sqrt{2}$ $x = 10$; and in curve 3, $a = 4$, $x = 5$; in all three curves $L = 3{\cdot}8317$, $q = 0$ (a, b, x, L non-dimensional).

When b is large the wave crests will presumably lie more or less parallel to the y-axis in the lee of the highest part of the mountain, with half-wedge effects at each end where the mountain is not so high.

The wavelength, λ, of the waves in the plane $y = 0$ (66) is $2\pi/\xi_n$, if we neglect the dependence of θ on x, which has little effect. The way in which λ varies as the characteristics of the undisturbed air stream, L and q, are changed is shown in figure 10. It appears that a small increase in q for a fixed value of L has little effect on the short wavelengths, but increases long wavelengths considerably; if q is increased sufficiently the wavelength may become so long that the disturbance is no longer observable as waves. A small increase of L for a fixed value of q decreases long wavelengths, but again has little effect on short wavelengths.

All the waves calculated in this paper, including those when l^2 is constant (§3), show the same behaviour with increase of a, the parameter governing the width of the mountain in the stream direction. This behaviour is given by the factor $a \exp(-\frac{1}{4}a^2\xi_n^2)$ in the amplitude (with $\xi_n = \xi_0$ ($= 1$ when $q = 0$, $y = 0$) in §3). If the mountain height H is kept constant the wave amplitude has a maximum value at $a = \sqrt{2}/\xi_n$; if H and a are varied in proportion, keeping the mountain the same shape, the amplitude is maximum at $a = 2/\xi_n$. The amplitude falls off rapidly on either side of these maxima. This 'resonance' of the waves when the wavelength is in the correct relationship with the mountain width was first pointed out by Corby & Wallington (1956) for two-dimensional waves. Curves of amplitude against a are shown for cases similar to the present one in I (figures 5 and 6).

Provided that a is not too small the factor $\exp(-\frac{1}{4}a^2\xi_n^2)$ also dominates the amplitude of (66) when considered as a function of L or of q. Increasing L for fixed q increases ξ_n and therefore decreases the amplitude in general, although if L increases from one of the critical values for which $\xi_n = 0$, the amplitude may increase at first. Thus as a function of L, maximum amplitude will occur near to the critical value; we must remember that ξ_n is not allowed to be too small, to prevent the pole from being close to the branch point at the origin. Increasing q from zero for a fixed L decreases ξ_n and so increases the amplitude initially,

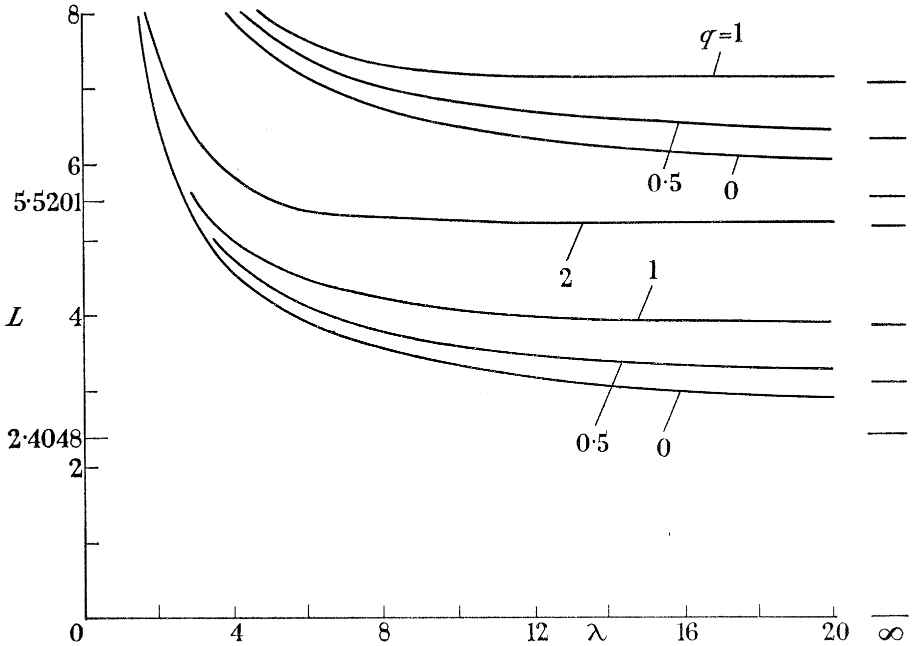

FIGURE 10. The wavelength in the plane $y = 0$, λ, as a function of L and q. If $q = 0$ we have no waves for $L \leqslant 2{\cdot}4048$, one wave for $2{\cdot}4048 < L \leqslant 5{\cdot}5201$, and two waves for $L > 5{\cdot}5201$, with similar ranges for other values of q (λ, L, q non-dimensional).

but as q approaches the limiting value which makes ξ_n zero the amplitude falls rapidly to zero. This is because $\xi_n^2\xi_n'' \to \infty$ as $\xi_n \to 0$. The function ξ_n'' can be found by differentiating (60) with respect to η and then putting $\xi_n'(\eta) = \eta = 0$, for the point corresponding to waves in the plane $y = 0$. This gives

$$\xi_n'' = -\frac{1}{\xi_n} - \frac{L\surd(\xi_n^2+q^2)}{\xi_n^3}\left\{\frac{\partial J_\nu(Z)/\partial Z}{\partial J_\nu(Z)/\partial\nu}\right\}_{Z=L,\,\nu=\surd(\xi_n^2+q^2)}. \tag{73}$$

If b is infinite and we have the ridge solution, ξ_n'' disappears from the wave term, and then the amplitude becomes infinite as q approaches the limiting value. As q is not allowed to be near these limiting values, we can say that increasing q usually increases the amplitude, the rate of increase depending on a, b and L.

The variation of the amplitude with height, z, is shown in figure 11, again for the plane $y = 0$. Curve 1 of figure 11 is for $L = 3{\cdot}8317$ ($\surd(\xi_n^2+q^2) = 1$). For this value the amplitude reaches a maximum at $z \doteq 0{\cdot}75$, above which it falls off rapidly. Curves 2 and 3 show the amplitudes of the two lee waves given by $L = 6{\cdot}379$ ($\surd(\xi_n^2+q^2) = 3$ or $0{\cdot}56$). The total lee wave for this value of L will be the sum of these two waves. From figure 11 we can see that the longer wavelength (curve 3) will be dominant for $z > 1$, say, but at low levels the dominant wave will be determined by the width a of the mountain, as either wave, but not both waves together, can be in resonance; if the mountain width is between the two resonance values the lee wave will be composed of each wavelength in roughly equal proportions. The curves of figure 11 apply also for waves in the lee of a ridge.

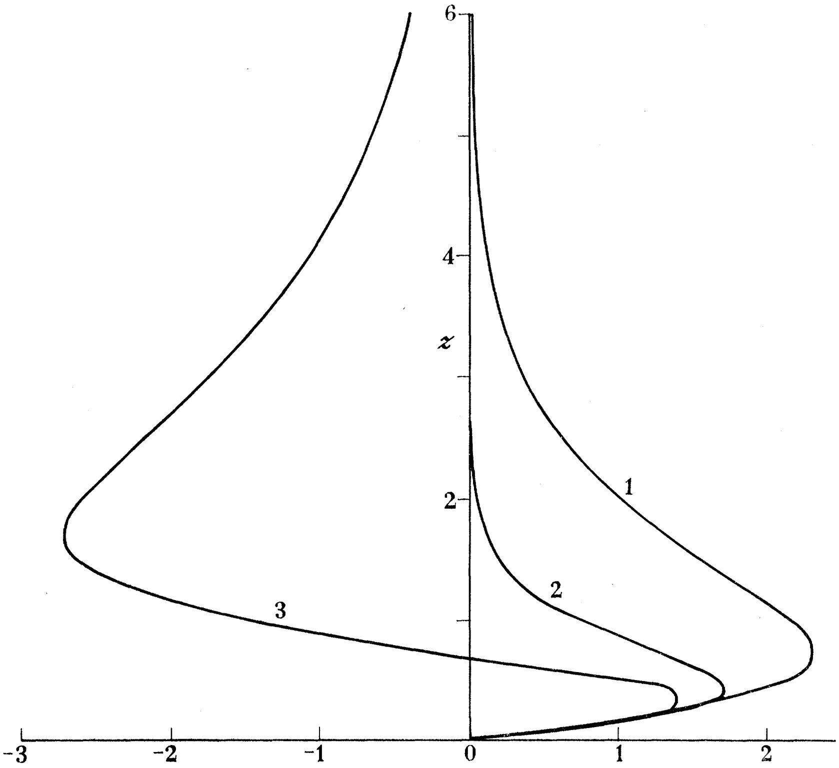

FIGURE 11. Wave amplitude in the plane $y = 0$ as a function of height z, for (1) $L = 3{\cdot}8317$ (1st zero); (2) $L = 6{\cdot}379$ (1st zero); (3) $L = 6{\cdot}379$ (2nd zero); with velocity and density assumed constant (z, L non-dimensional).

The actual waves formed in the plane $y = 0$ when $L = 3{\cdot}8317$, $q = 0$ are shown in figure 12 for a circular mountain with $a = b = \surd 2$, $H = \frac{1}{2}$ and for the corresponding ridge $a = \surd 2$, $b = \infty$, $H = \frac{1}{2}$. The velocity and density are taken to be constant. The non-dimensional wavelength in this case is approximately 2π. The values of h used by Palm & Foldvik (1960) are in the range of $2{\cdot}5 \times 10^3$ to 3×10^4 m, which makes the actual value of the wavelength lie between about 15 and 200 km. Obviously the largest values of h give waves which for this value of L are much too long to be of interest in our problem, and in which the effects of the earth's rotation will appear. The waves at height $z = 0{\cdot}75$ in figure 12 are the waves of maximum amplitude with regard to height, and all waves have the maximum amplitude for this height of mountain, because $a\xi_n = \surd 2$. Since the two-dimensional waves cut the ground, which is another streamline, it is clear that the linear theory does not apply to mountains as high as $H = \frac{1}{2}$ when $a = \surd 2$, $b = \infty$, the wave amplitude being simply proportional to H.

The waves for $z = 3$, $y = 0$, with $a = \surd 2$, $H = \frac{1}{2}$, as in figure 12, have also been calculated for the case of constant l^2 with $q = 0$, from (46), approximated for $xb^2 \gg 2z^2$ ($b > 5$). The

PHILOSOPHICAL TRANSACTIONS OF THE ROYAL SOCIETY A MATHEMATICAL, PHYSICAL & ENGINEERING SCIENCES

amplitude of the first wave, which has its crest at $x \simeq 6$, is about the same as the amplitude of the first wave of the exponential l^2 case at the same height ($z = 3$) for the circular mountain, but when l^2 is constant the rate of decay is increased. As the amplitude increases linearly with height when l^2 is constant, the waves are very much smaller than the waves of figure 12 at height $z = 0{\cdot}75$ but are beginning to have a non-negligible amplitude at the height at which the theory of § 3 breaks down.

The shape of the wave crests for the exponential l^2 case with $L = 3{\cdot}8317$, $q = 0$, calculated from the doublet solution by the method of figure 8, is shown in figure 13. The phase difference of $\frac{1}{2}\pi$ between the two sets of waves is due to the change of sign of ξ''_{nn} (see (71)) at the point of inflexion of $\xi_n(\eta)$. At the edges of the wedge the waves are actually a single system,

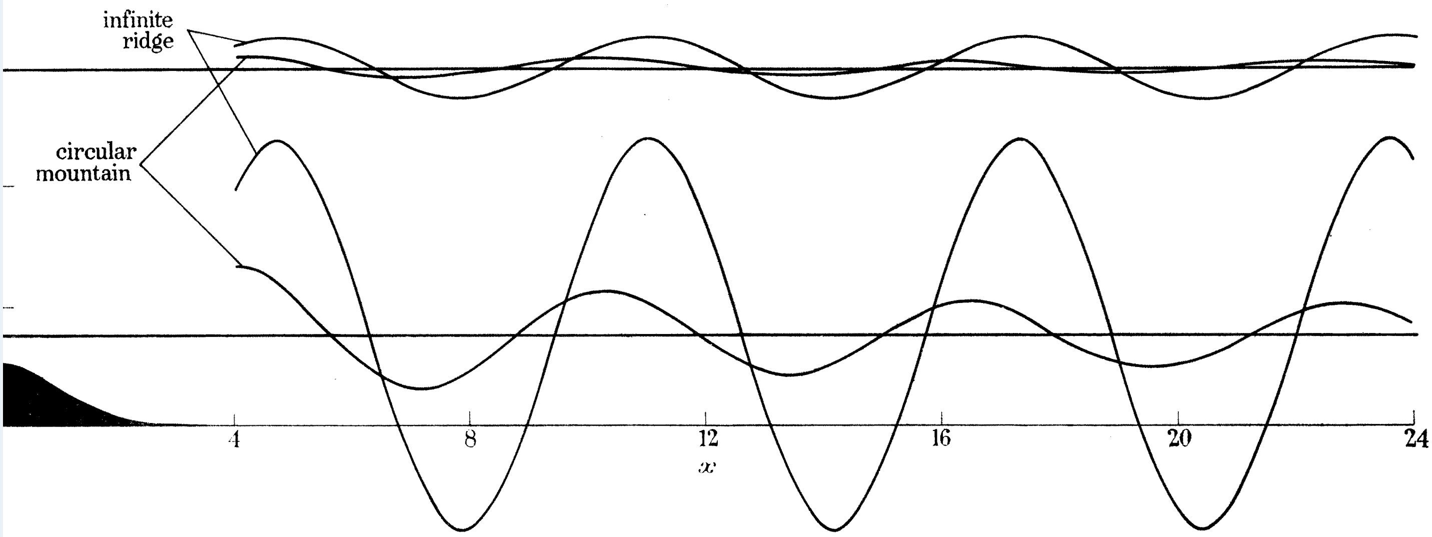

FIGURE 12. Waves in the plane $y = 0$ for the circular mountain with $a = b = \sqrt{2}$, $H = \frac{1}{2}$, and for the infinite ridge $a = \sqrt{2}$, $b = \infty$, $H = \frac{1}{2}$, when $L = 3{\cdot}8317$ and velocity and density are assumed constant (a, b, H, x, z, L non-dimensional). The scale of the mountain and the waves is the same as that of the height, z, of the undisturbed streamlines. Since the waves given by the ridge cut the ground, the theory will not apply to ridges as high as $H = \frac{1}{2}$ when $a = \sqrt{2}$; in this case the mountain shape and waves may be taken to be for a smaller H, but drawn on a larger scale than that of z.

with crests mid-way between those shown (from (72)). The position of the point of inflexion in the curve $\xi = \xi_n(\eta)$ for this value of L (figure 6) has not been determined accurately, and therefore the semi-angle of the wedge, which measures $23\frac{1}{2}°$, is not accurate. The same wedge angle applies at all heights, but will change if L changes. For $L = 3{\cdot}4910$, $q = 0$ ($\xi_n = 0{\cdot}75$) the semi-angle is approximately $28\frac{1}{2}°$. Considering this and also the curves of figure 7, it appears that the wedge angle decreases as L increases (wavelength decreases) for the waves from the first pole; waves from the second pole, when they exist, are contained in a wedge with a wider angle than that of the wedge containing the waves from the first pole.

In view of their similarity to water waves, the waves given when l^2 is exponential are just as expected. The waves given when l^2 is constant are very unusual, particularly the behaviour of the amplitude as a function of b, coupled with waves contained in a strip and not in a wedge, and the dependence on q. Clearly some physical explanation of these results is desirable, but at the present time no such explanation is offered. The difference between the waves contained in a strip and those contained in a wedge will be essentially mathematical, however, because, as remarked earlier, only the transverse system of waves will be detectable in the wedge cases, and these waves will appear to be within a strip.

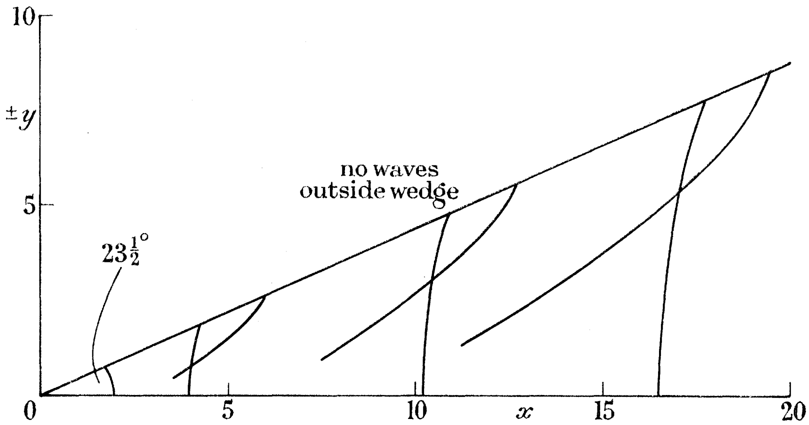

FIGURE 13. Wave crests in horizontal planes as shown by the 'doublet' solution, for $L = 3{\cdot}8317$, $q = 0$ (x, y, L non-dimensional).

REFERENCES

Beckmann, P. & Franz, W. 1957 *Z. angew. Math. Mech* **37**, 17.
Corby, G. A. & Sawyer, J. S. 1958*a* *Quart. J. R. Met. Soc.* **84**, 25.
Corby, G. A. & Sawyer, J. S. 1958*b* *Quart. J. R. Met. Soc.* **84**, 284.
Corby, G. A. & Wallington, C. E. 1956 *Quart. J. R. Met. Soc.* **82**, 266.
Crapper, G. D. 1959*a* (I) *J. Fluid Mech.* **6**, 51.
Crapper G. D. 1959*b* Ph.D. Thesis, Manchester University.
Eliassen, E. & Palm, E. 1954 *Inst. Weather and Climate Res.* (*Oslo.*), *Publ.* no. 1.
Höiland, E. 1951 *Sierra Wave Project, Progr. Rep. no.* 5, *appendix A*, Dep. Met. Univ. Calif.
Lighthill, M. J. 1960 *Phil. Trans.* A, **252**, 397.
Long, R. R. 1953 *Tellus*, **5**, 42.
Long, R. R. 1955 *Tellus*, **7**, 341.
Palm, E. 1953 *Astrophys. Norveg.* **5**, no. 3, Oslo.
Palm, E. 1958 *Geofys. Publ.* (*Oslo*), **20**, no. 3.
Palm, E. & Foldvik, A. 1960 *Geofys. Publ.* (*Oslo.*), **21**, no. 6.
Sawyer, J. S. 1960 *Quart. J. R. Met. Soc.* **86**, 326.
Scorer, R. S. 1949 *Quart. J. R. Met. Soc.* **75**, 41.
Scorer, R. S. 1958*a* *Quart. J. R. Met. Soc.* **84**, 182.
Scorer, R. S. 1958*b* *Quart. J. R. Met. Soc.* **84**, 465.
Scorer, R. S. & Klieforth, H. 1959 *Quart. J. R. Met. Soc.* **85**, 131.
Scorer, R. S. & Wilkinson, M. 1956 *Quart. J. R. Met. Soc.* **82**, 419.
Stoker, J. J. 1953 *Commun. Pure App. Maths.* **6**, 471.
Watson, G. N. 1944 *A treatise on the theory of Bessel functions*, 2nd ed. Cambridge University Press.
Wurtele, M. G. 1953 *Sierra Wave Project, Sci. Rep. no.* 3, Dep. Met. Univ. Calif.
Wurtele, M. G. 1955 *J. Mar. Res.* **14**, 1.
Wurtele, M. G. 1957 *Beitr. Phys. Atmos.* **29**, 242.
Yih, C-S. 1960*a* *J. Fluid Mech.* **8**, 481.
Yih, C-S. 1960*b* *J. Fluid Mech.* **9**, 68.
Yih, C-S. 1960*c* *J. Fluid Mech.* **9**, 161.